

1 Article

2 Biochemical properties of a decoy 3 oligodeoxynucleotide inhibitor of STAT3 transcription 4 factor

5 **David S. Lee** ¹, **Rachel A. O'Keefe** ², **Patrick K. Ha** ², **Jennifer R. Grandis** ², and **Daniel E. Johnson** ^{2*}

6 ¹ School of Medicine, University of California at San Francisco, San Francisco, CA, USA

7 ² Department of Otolaryngology – Head and Neck Surgery, University of California at San Francisco, San
8 Francisco, CA, USA

9 * Correspondence: Daniel.Johnson@ucsf.edu

10

11 **Abstract:** Cyclic STAT3 decoy (CS3D) is a second-generation, double-stranded oligodeoxynucleotide
12 (ODN) that mimics a genomic response element for signal transducer and activator of transcription 3
13 (STAT3), an oncogenic transcription factor. CS3D competitively inhibits STAT3 binding to target gene
14 promoters, resulting in decreased expression of proteins that promote cellular proliferation and
15 survival. Previous studies have demonstrated antitumor activity of CS3D in preclinical models of
16 solid tumors. However, prior to entering human clinical trials, the efficiency of generating the CS3D
17 molecule and its stability in biological fluids should be determined. CS3D is synthesized as a
18 single-stranded ODN and must have its free ends ligated to generate the final cyclic form. In this
19 study, we report a ligation efficiency of nearly 95 percent. The ligated CS3D demonstrated a half-life
20 of 7.9 hours in human serum, indicating adequate stability for intravenous delivery. These results
21 provide requisite biochemical characterization of CS3D that will inform upcoming clinical trials.

22 **Keywords:** STAT3 as a drug target; cyclic STAT3 decoy; oligodeoxynucleotide inhibitor; head and
23 neck cancer

24

25 1. Introduction

26 Signal transducer and activator of transcription 3 (STAT3) is a highly regulated transcription
27 factor that plays a prominent role in cellular growth and survival, as well as inflammation [1-2].
28 STAT3 is activated by phosphorylation of tyrosine 705 by upstream kinases, including Janus kinases
29 (JAKs). Phosphorylation of STAT3 leads to homodimerization, translocation to the nucleus, and
30 induction of target gene expression. In normal cells, activation of STAT3 is typically transient.
31 However, constitutive hyperactivation of STAT3 has been observed in multiple human cancers,
32 where it contributes to tumor development [3-4]. Additionally, STAT3 signaling promotes resistance
33 to conventional chemoradiation and small-molecule inhibitors of other oncogenic signaling pathways
34 [5-11]. Not surprisingly, aberrant activation of STAT3 has been shown to correlate with poor clinical
35 prognosis in a number of malignancies [12-14]. Preclinical studies indicate that knockdown or
36 inhibition of STAT3 selectively causes apoptosis in cancerous cells and rescues sensitivity to the
37 aforementioned therapies [3,4,15-17]. By contrast, abrogation of STAT3 signaling is substantially less
38 deleterious to non-cancerous cells, at least in healthy adults [2,18]. In view of the pivotal role of
39 STAT3 in human malignancies, a concerted effort has been made over the past two decades to
40 develop selective inhibitors of STAT3 signaling.

41 The blockade of upstream kinases (e.g., JAKs) is a well-validated strategy for inhibiting STAT3
42 activation and inducing anti-cancer effects [9,19-23]. Indeed, most currently advertised STAT3
43 inhibitors target upstream activators. More recently, pharmaceuticals have been developed that
44 interfere with expression of the STAT3 protein [22,24]. Among these is AZD9150, a modified
45 antisense oligodeoxynucleotide (ODN) that targets *STAT3* mRNA for destruction. AZD9150 has
46 shown promise in early clinical trials, reducing tumor burden in patients with refractory lymphoma
47 and non-small cell lung cancer [24]. It is currently being evaluated as monotherapy in patients with
48 advanced solid tumors and in combination with chemotherapy and/or durvalumab, an anti-PD-L1
49 monoclonal antibody (NCT: 03421353).

50 STAT3 decoys utilize a distinct mechanism of action to inhibit signaling via the STAT3 pathway.
51 Based on a genomic response element bound by activated STAT3, the decoy molecules bind and
52 inhibit STAT3 dimers. A first-generation STAT3 decoy (S3D) was a linear double-stranded ODN, 15
53 base pairs in length with free ends. This linear S3D inhibits the growth of solid tumors in preclinical
54 models and is well-tolerated in preclinical models [21,25-29]. In a Phase 0 clinical trial, intratumoral
55 injection of the linear S3D decreased expression of the STAT3 target genes encoding anti-apoptotic
56 Bcl-XL and pro-proliferative cyclin D1 [30]. In an effort to develop a STAT3 decoy formulation more
57 resistant to degradation by nucleases and, thereby, amenable to systemic delivery, hexaethylene
58 glycol spacers were covalently attached to the free ends of linear S3D to create the second-generation
59 cyclic STAT3 decoy (CS3D) [30]. Although CS3D has demonstrated similar biological activity and
60 safety as its linear predecessor, the stability of CS3D in human serum has not been determined
61 [26,30]. In the present study, we investigated the biochemical properties of CS3D. Since complete
62 cyclization of CS3D requires an enzymatic ligation step, we first determined the efficiency of this
63 ligation process. A biotinylated version of the CS3D was also generated, allowing pull-down of intact
64 CS3D from human serum samples and determination of stability. Our results demonstrate that CS3D
65 exhibits a roughly three-fold longer half-life in human serum compared to the first-generation linear
66 S3D, an improvement that will facilitate more effective systemic delivery in humans.

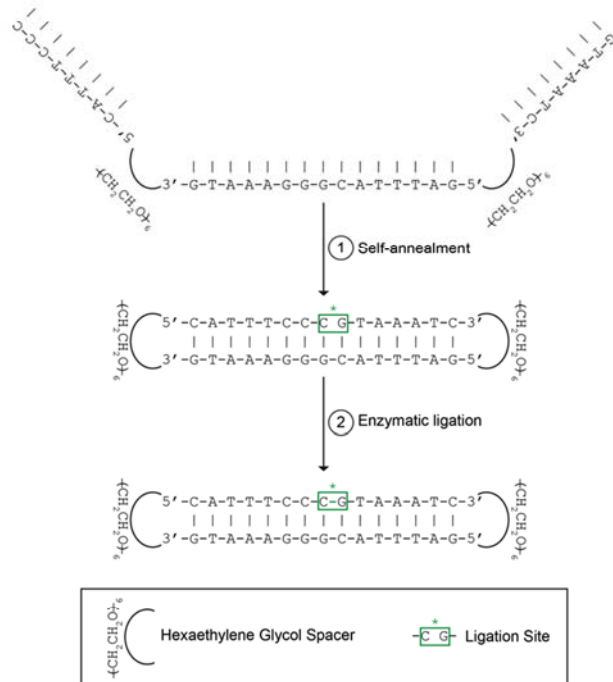
67 2. Results

68 2.1. Efficient Ligation of CS3D

69 CS3D is initially synthesized as a unimolecular, single-stranded sequence. Following
70 self-annealing at room temperature, enzymatic ligation with T4 DNA ligase is performed to generate
71 the completely cyclic molecule, CS3D (Figure 1A). To investigate the efficiency and consistency of the
72 ligation process, we performed multiple ($n = 5$) small-volume ligations using the same drug stock and
73 identical reaction conditions. Aliquots from each ligation reaction were then subjected to
74 electrophoresis on urea/polyacrylamide gels, followed by staining with SYBR Gold and quantification
75 of band intensity. On average, CS3D was ligated with 94.7 ± 0.5 percent efficiency (Figure 1B). These
76 results suggest that cyclization of CS3D through enzymatic ligation is a consistent and reproducible
77 process.

Figure 1

A



B

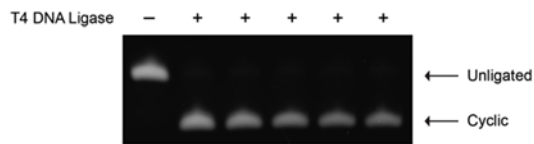
78
79
80
81
82
83
84
85
86

Figure 1. Efficient ligation of cyclic STAT3 decoy (CS3D). (A) Schematic representation of CS3D ligation with T4 DNA ligase. The complementary segments of the single-stranded decoy molecule spontaneously self-anneal. Enzymatic ligation with T4 DNA ligase was used to complete cyclization. (B) Incubations were performed in the absence or presence of T4 DNA ligase overnight. Multiple identical ligations ($n = 5$) were simultaneously performed. Samples from each reaction were then electrophoresed on a urea/polyacrylamide gel, stained with SYBR Gold, and quantified by densitometry.

87
88
89
90
91
92
93
94
95
96

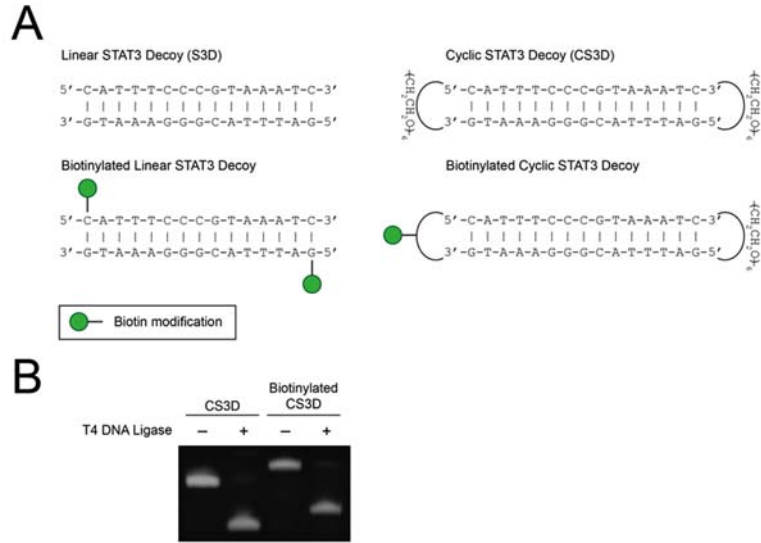
2.2. Biotinylation of CS3D Does Not Affect Ligation Efficiency

After establishing minimal variability between CS3D enzymatic ligations, we sought to compare the stabilities of linear and cyclic STAT3 decoys in human serum. Previous studies have shown that covalent modifications to the terminal nucleotides of ODN decoys protect against serum nucleases [31-34]. We hypothesized that flanking linear S3D with hexaethylene glycol spacers and subsequent cyclization would shield the free ends from nucleolytic degradation in human serum (Figure 2A). To enable quantitative determination of decoy levels in human serum, we developed a pull-down assay to purify the decoys from the serum samples. The assay utilized streptavidin-conjugated agarose resin to efficiently pull down biotinylated versions of S3D or CS3D. In preliminary experiments, we first evaluated whether biotinylation would affect enzymatic ligation of

97 CS3D. As expected, biotinylation increased the molecular weight of CS3D, but had no observable
98 impact on ligation efficiency (Figure 2B).

99

Figure 2



100

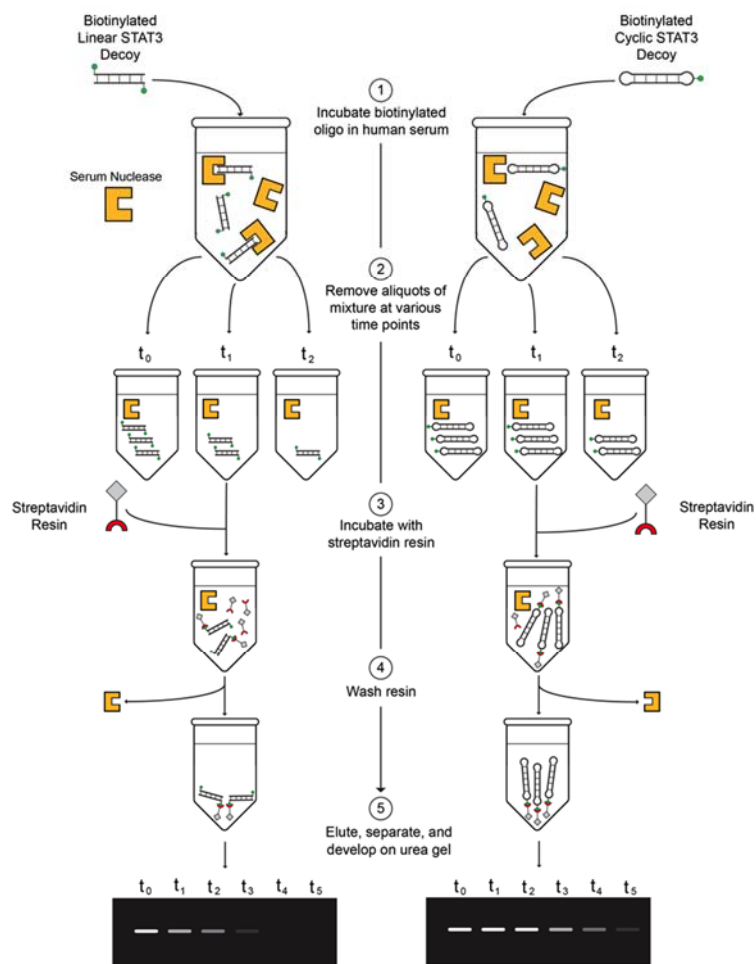
Figure 2. Ligation of CS3D is unaffected by biotinylation. (A) Structures of parental and biotinylated S3D and CS3D. (B) CS3D and biotinylated CS3D were incubated with T4 DNA ligase overnight, followed by electrophoresis on a urea/polyacrylamide gel and staining with SYBR Gold.

105

106 2.3 CS3D Demonstrates Greater Stability in Human Serum than Linear STAT3 Decoy (S3D)

To determine the stabilities in human serum of the linear first-generation and cyclic second-generation STAT3 decoys, the biotinylated decoys were incubated in fresh human serum for varying lengths of time, pulled down with streptavidin-agarose resin, and then analyzed on urea/polyacrylamide gels (Figure 3). Serum stability assays were performed in two different human serum samples for more reliable assessment of decoy half-lives (Figure 4A-D). The linear S3D exhibited an average half-life of 2.5 ± 1.2 hours in the two serum samples (1.7 h in serum sample #1; 3.4 h in serum sample #2). CS3D, on the other hand, exhibited markedly enhanced resistance to degradation with an average half-life of 7.9 ± 2.0 hours (6.5 h in serum sample #1; 9.3 h in serum sample #2). These findings underscore the improved stability of CS3D and its potential for clinical application as a systemically delivered agent.

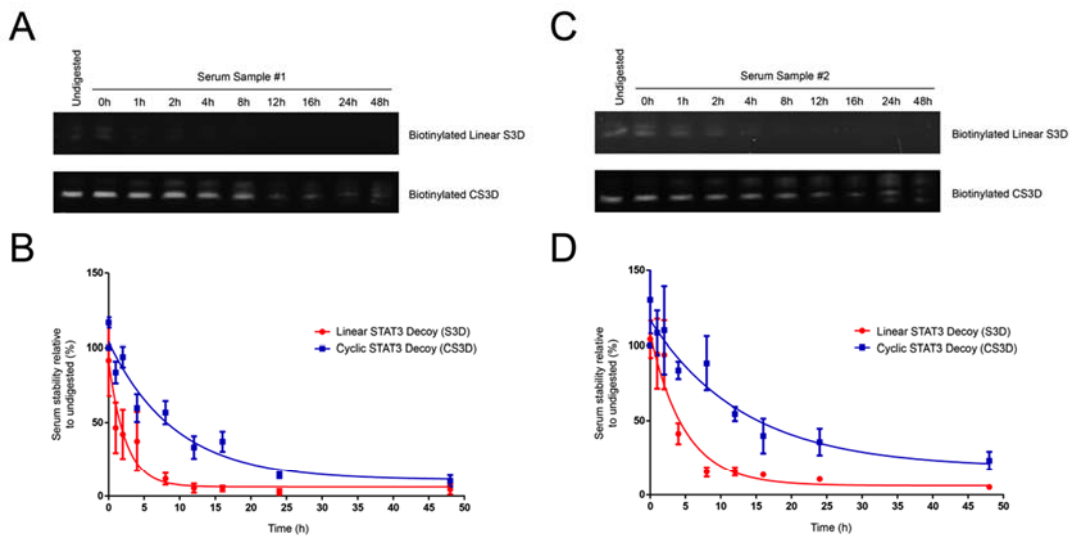
Figure 3.



117
118
119
120
121
122
123

Figure 3. Diagram of the serum stability assay. (1) Incubate biotinylated ODN in fresh human serum. (2) Remove aliquots of ODN/serum mixture at various time points and store in -80°C. (3) Incubate streptavidin resin with thawed aliquots of ODN/serum mixture. (4) Pellet and wash three times. (5) Elute by boiling, separate on urea/polyacrylamide gels, and develop with ultraviolet light.

Figure 4



124
125
126
127
128
129
130
131
132

Figure 4. CS3D exhibits a longer half-life in human serum than linear S3D. (A, C) Biotinylated S3D and CS3D were incubated in human serum samples #1 or #2 and aliquots were removed at varying time intervals, electrophoresed on urea/polyacrylamide gels, and stained with SYBR Gold. (B, D) Densitometric analyses were performed on biotinylated S3D and CS3D pulled down from serum. Stability at each time point was expressed as a percent relative to its respective “undigested” control. Undigested control represents decoy suspended in 1X phosphate-buffered saline (PBS) and lacking any serum. Each time point of the S3D and CS3D serum stability assays was performed in triplicate for each sample of human serum.

133 **3. Discussion**

134 Numerous solid tumor malignancies have been shown to exhibit oncogenic dependency on
135 STAT3 [35,36]. However, no direct STAT3 inhibitors are currently used in clinical practice. Cyclic
136 STAT3 decoy (CS3D), a double-stranded oligodeoxynucleotide (ODN) that competitively inhibits
137 STAT3 binding to genomic response elements, has been shown to exert selective cytotoxicity against
138 cancers with hyperactivated STAT3 [26,30,37]. To date, the stability of CS3D in human serum has
139 remained unknown. In this study, we utilized a novel pull-down approach to measure the serum
140 stabilities of CS3D, as well as an earlier linear version of the STAT3 decoy. By comparing the
141 respective half-lives of the cyclic and linear STAT3 decoys, we determined that cyclization resulted in
142 substantially improved stability in human serum. We further determined that the process of
143 enzymatic ligation used to generate the cyclized CS3D is highly efficient and can likely be scaled up
144 to generate large quantities of the inhibitor. Translating CS3D to the clinic will augment current
145 treatment strategies for cancers that are characterized by dependence on STAT3 signaling. Moreover,
146 successful application of CS3D will provide a foundation for the development and use of ODN
147 decoys to target transcription factors in disease states including and beyond cancer.

148 Transcription factor decoys comprise a class of nucleic acid-based agents that modulate the
149 cellular activity of transcription factors, proteins that are often considered undruggable [38]. Decoys
150 are short double-stranded ODNs designed to mimic the genomic sequences in target gene promoters
151 that are recognized by transcription factors [39]. Although decoys have been studied in clinical trials
152 for venous bypass graft vasculopathy and head and neck squamous cell carcinoma (HNSCC),
153 instability represents a major translational hurdle because extracellular and intracellular nucleases
154 rapidly degrade the free ends of linear ODN decoys [30, 40-42]. In an effort to minimize such
155 degradation, modifications at the free ends of decoy ODNs have been used to improve resistance
156 against enzymatic activity. These modifications include the use of phosphorothioate linkers,
157 unnatural nucleotides, and polyethylene glycol attachments [31-34]. Prior studies to assess the
158 stabilities of modified ODNs have primarily focused on laboratory-generated aqueous solutions
159 containing defined levels of human nucleases, whereas the current study assessed decoy stability in
160 human serum samples. Moreover, we developed and utilized a novel pull-down assay, allowing us to
161 easily purify intact, biotinylated decoys from the serum. Our findings of improved stability with the
162 cyclic STAT3 decoy confirm the value of modifying or removing the free ends of decoy ODNs.

163 Although our results suggest that CS3D may be amenable to intravenous delivery in humans, the
164 optimal approach for targeted delivery to diseased tissue remains unclear. Strategies that have been
165 developed to enhance delivery include topical ointments, and the use of glycopolymers and
166 nanoparticles, among others [43-45]. Another method that has proven successful involves the use of
167 an ultrasound-targeted microbubble destruction (UTMD) system [46]. In this system, ODNs are
168 packaged into microbubbles that are delivered intravenously. An external ultrasound probe at the
169 desired delivery site facilitates rupture of the microbubbles, resulting in localized delivery. A
170 previous study using UTMD-mediated delivery of CS3D has demonstrated intratumoral uptake in a
171 murine model [47].

172 In summary, the use of cyclic ODN decoys may provide an effective strategy for targeting
173 transcription factors, including STAT3. However, no transcription factor decoys have yet been
174 translated to clinical practice. Our results reveal that fully cyclized CS3D can be efficiently generated
175 via enzymatic ligation. Moreover, CS3D demonstrates improved stability in human serum relative to
176 linear decoy with free ends. These findings will facilitate further clinical development of CS3D and
177 provide evidence supporting the potential use of transcription factor decoys as viable therapeutic
178 agents.

179 **4. Materials and Methods**

180 *4.1 Synthesis of Biotinylated Linear STAT3 Decoy (S3D) and Biotinylated Cyclic STAT3 Decoy (CS3D)*

181 Biotinylated linear S3D was synthesized as two complementary single-stranded
182 oligodeoxynucleotides (ODNs) by Sigma-Aldrich (St. Louis, MO, USA). Biotinylated CS3D was
183 synthesized as a unimolecular single-stranded ODN by Integrated DNA Technologies (Skokie, IL,
184 USA). S3D and CS3D were reconstituted in normal saline as 800 μ M stock solutions and stored at
185 -20°C.

186

187 *4.2 Ligation of Cyclic STAT3 Decoy (CS3D) and Biotinylated CS3D*

188 15 μ L of single-stranded oligodeoxynucleotides (ODN) were incubated with 3 μ L of T4 DNA
189 ligase (400,000 U/mL; New England BioLabs, M0202S) and 2 μ L of 10X T4 DNA ligase reaction buffer

190 (New England BioLabs, B0202S) overnight at room temperature. Ligated material was subsequently
191 diluted to 1 μ M, incubated with DNA loading buffer at 60°C for 5 minutes, and electrophoresed on
192 15% Tris-Borate-EDTA (TBE) urea/polyacrylamide gels. The ODNs were detected by incubating gels
193 in 1X SYBR Gold solution (Thermo Fisher Scientific, S11494) for 1 hour at 4°C in the dark, followed by
194 exposure to ultraviolet light and image detection using Azure c600 (Biosystems, Dublin, CA, USA).
195 The relative densities of ligated and unligated ODN bands were quantified using Image Studio Lite
196 v5.2.5 (LI-COR Biosciences, Lincoln, NE, USA).

197

198 *4.3 Annealing of Biotinylated Linear STAT3 Decoy (S3D)*

199 Complementary sense and antisense strands of biotinylated linear S3D were incubated in
200 equimolar concentrations at 100°C for 1 hour, followed by annealing at room temperature overnight.
201 The annealed oligodeoxynucleotides (ODN) were stored at 4°C.

202

203 *4.4 Serum Stability Assay*

204 The stability of biotinylated ODNs in human serum was determined following incubation and
205 pull-down of the intact ODN [30,48]. Briefly, human serum was obtained from two individuals in
206 compliance with the Institutional Review Board of the University of California, San Francisco (IRB
207 #14-15342). Biotinylated ODNs were incubated in 100% human serum at a final concentration of 0.05
208 μ g/mL. After varying lengths of time, aliquots (20 μ L) were removed and immediately stored at -80°C.
209 After the final time point, each aliquot was incubated with streptavidin-coated agarose resin (Pierce
210 Streptavidin Resin, Thermo Fisher Scientific, 20347) for 60 minutes at room temperature, pelleted by
211 centrifugation, and washed 3 times in 3X phosphate-buffered saline (PBS) containing 0.05%
212 Tween-20. The pelleted resin was then resuspended in DNA loading buffer, followed by heating at
213 95°C for 4 minutes to elute the ODNs. Supernatants were electrophoresed on 15% TBE
214 urea/polyacrylamide gels and visualized as described above. The optical densities of the samples
215 were compared to the optical densities of corresponding biotinylated ODNs suspended in 1X PBS
216 that were not incubated in serum.

217

218 *4.5 Statistical Analysis*

219 Analyses of the serum stabilities of S3D and CS3D were performed using GraphPad Prism 5.04
220 (La Jolla, CA, USA).

221 **Author Contributions:**

222 David Lee, Rachel O'Keefe, Jennifer Grandis, and Daniel Johnson conceived and designed the experiments;
223 David Lee and Rachel O'Keefe performed the experiments; David Lee performed data analysis; David Lee wrote
224 the manuscript; Rachel O'Keefe, Daniel Johnson, Jennifer Grandis, and Patrick Ha assisted with writing and
225 proofreading.

226 **Funding:**

227 This work was funded by National Institutes of Health grants R01 DE024728 (DEJ), P50CA097190 (DEJ and
228 JRG), and R01 DE023685 (JRG); and American Cancer Society grant CRP-13-308-06-COUN (JRG).

229 **Conflicts of Interest:**

230 The authors declare no conflict of interest. The funding sponsors had no role in the design of the study; in
231 the collection, analyses, or interpretation of data; in the writing of the manuscript, and in the decision to publish
232 the results.

233 **Abbreviations**

S3D	linear STAT3 decoy
CS3D	cyclic STAT3 decoy
ODN	oligodeoxynucleotide
STAT3	signal transducer and activator of transcription 3
JAK	Janus kinase
HNSCC	head and neck squamous cell carcinoma
UTMD	ultrasound-targeted microbubble destruction
PBS	phosphate-buffered saline

234 **References**

1. Yu, H.; Pardoll, D.; Jove, R. STATs in cancer inflammation and immunity: a leading role for STAT3. *Nat. Rev. Cancer* **2009**, *9*, 798–809.
2. Yu, H.; Jove, R. The STATs of cancer--new molecular targets come of age. *Nat. Rev. Cancer* **2004**, *4*, 97–105.
3. Darnell, J. E. Validating Stat3 in cancer therapy. *Nat. Med.* **2005**, *11*, 595–596.
4. Germain, D.; Frank, D. a. Targeting the cytoplasmic and nuclear functions of signal transducers and activators of transcription 3 for cancer therapy. *Clin. Cancer Res.* **2007**, *13*, 5665–5669.
5. Chen, M. F.; Chen, P. T.; Lu, M. S.; Lin, P. Y.; Chen, W. C.; Lee, K. D. IL-6 expression predicts treatment response and outcome in squamous cell carcinoma of the esophagus. *Mol Cancer* **2013**, *12*, 26.
6. Kim, K. W.; Mutter, R. W.; Cao, C.; Albert, J. M.; Shinohara, E. T.; Sekhar, K. R.; Lu, B. Inhibition of signal transducer and activator of transcription 3 activity results in down-regulation of Survivin following irradiation. *Mol. Cancer Ther.* **2006**, *5*, 2659–2665.
7. Kim, S. M.; Kwon, O.-J.; Hong, Y. K.; Kim, J. H.; Solca, F.; Ha, S.-J.; Soo, R. A.; Christensen, J. G.; Lee, J. H.; Cho, B. C. Activation of IL-6R/JAK1/STAT3 Signaling Induces De Novo Resistance to Irreversible EGFR Inhibitors in Non-Small Cell Lung Cancer with T790M Resistance Mutation. *Mol. Cancer Ther.* **2012**, *11*, 2254–2264.
8. Prahallad, A.; Sun, C.; Huang, S.; Di Nicolantonio, F.; Salazar, R.; Zecchin, D.; Beijersbergen, R. L.; Bardelli, A.; Bernards, R. Unresponsiveness of colon cancer to BRAF(V600E) inhibition through feedback activation of EGFR. *Nature* **2012**, *483*, 100–104.
9. Vultur, A.; Villanueva, J.; Krepler, C.; Rajan, G.; Chen, Q.; Xiao, M.; Li, L.; Gimotty, P. A.; Wilson, M.; Hayden, J.; Keeney, F.; Nathanson, K. L.; Herlyn, M. MEK inhibition affects STAT3 signaling and invasion in human melanoma cell lines. *Oncogene* **2014**, *33*, 1850–1861.
10. Spitzner, M.; Ebner, R.; Wolff, H. A.; Michael Ghadimi, B.; Wienands, J.; Grade, M. STAT3: A novel molecular mediator of resistance to chemoradiotherapy. *Cancers* **2014**, *6*, 1986–2011.
11. Wu, C. Te; Chen, M. F.; Chen, W. C.; Hsieh, C. C. The role of IL-6 in the radiation response of prostate cancer. *Radiat. Oncol.* **2013**, *8*.
12. Wen, W.; Wu, J.; Liu, L.; Tian, Y.; Buettner, R.; Hsieh, M.-Y.; Horne, D.; Dellinger, T. H.; Han, E. S.; Jove, R.; Yim, J. H. Synergistic anti-tumor effect of combined inhibition of EGFR and JAK/STAT3 pathways in human ovarian cancer. *Mol. Cancer* **2015**, *14*, 100.
13. Takemoto, S.; Ushijima, K.; Kawano, K.; Yamaguchi, T.; Terada, A.; Fujiyoshi, N.; Nishio, S.; Tsuda, N.; Ijichi, M.; Kakuma, T.; Kage, M.; Hori, D.; Kamura, T. Expression of activated signal transducer and activator of transcription-3 predicts poor prognosis in cervical squamous-cell carcinoma. *Br. J. Cancer* **2009**, *101*, 967–972.

269 14. Chen, C.-L.; Cen, L.; Kohout, J.; Hutzén, B.; Chan, C.; Hsieh, F.-C.; Loy, A.; Huang, V.; Cheng, G.;
270 Lin, J. Signal transducer and activator of transcription 3 activation is associated with bladder cancer
271 cell growth and survival. *Mol. Cancer* **2008**, *7*, 78.

272 15. Alas, S.; Bonavida, B. Inhibition of constitutive STAT3 activity sensitizes resistant non-Hodgkin's
273 lymphoma and multiple myeloma to chemotherapeutic drug-mediated apoptosis. *Clin. Cancer Res.*
274 **2003**, *9*, 316–326.

275 16. Rivat, C.; De Wever, O.; Bruyneel, E.; Mareel, M.; Gespach, C.; Attoub, S. Disruption of STAT3
276 signaling leads to tumor cell invasion through alterations of homotypic cell-cell adhesion
277 complexes. *Oncogene* **2004**, *23*, 3317–3327.

278 17. Zhang, X.; Sun, Y.; Pireddu, R.; Yang, H.; Urlam, M. K.; Lawrence, H. R.; Guida, W. C.; Lawrence,
279 N. J.; Sefti, S. M. A novel inhibitor of STAT3 homodimerization selectively suppresses STAT3
280 activity and malignant transformation. *Cancer Res.* **2013**, *73*, 1922–1933.

281 18. Schlessinger, K.; Levy, D. E. Malignant transformation but not normal cell growth depends on
282 signal transducer and activator of transcription 3. *Cancer Res.* **2005**, *65*, 5828–5834.

283 19. Johnston, P.; Grandis, J. STAT3 signaling: anticancer strategies and challenges. *Mol. Interventions*
284 **2011**, *11*, 18–26.

285 20. Wake, M. S.; Watson, C. J. STAT3 the oncogene - Still eluding therapy? *FEBS J.* **2015**, *282*, 2600–2611.

286 21. Sen, M.; Joyce, S.; Panahandeh, M.; Li, C.; Thomas, S. M.; Maxwell, J.; Wang, L.; Gooding, W. E.;
287 Johnson, D. E.; Grandis, J. R. Targeting Stat3 abrogates EGFR inhibitor resistance in cancer. *Clin.*
288 *Cancer Res.* **2012**, *18*, 4986–4996.

289 22. Yu, C.-L.; Jove, R.; Turkson, J. In *STAT Inhibitors in Cancer*; Ward, A., Ed.; Springer International
290 Publishing: Cham, Switzerland, **2016**; pp. 69–94.

291 23. Lee, D. S.; Grandis, J. R.; Johnson, D. E. In *Targeting Cell Survival Pathways to Enhance Response to*
292 *Chemotherapy*; Johnson, D. E., Ed.; Elsevier, **2018**.

293 24. Hong, D.; Kurzrock, R.; Kim, Y.; Woessner, R.; Younes, A.; Nemunaitis, J.; Fowler, N.; Zhou, T.;
294 Schmidt, J.; Jo, M.; Lee, S. J.; Yamashita, M.; Hughes, S. G.; Fayad, L.; Piha-Paul, S.; Nadella, M. V. V.
295 P.; Mohseni, M.; Lawson, D.; Reimer, C.; Blakey, D. C.; Xiao, X.; Hsu, J.; Revenko, A.; Monia, B. P.;
296 MacLeod, A. R. AZD9150, a next-generation antisense oligonucleotide inhibitor of STAT3 with
297 early evidence of clinical activity in lymphoma and lung cancer. *Sci. Transl. Med.* **2015**, *7*,
298 314ra185–314ra185.

299 25. Leong, P. L.; Andrews, G. a; Johnson, D. E.; Dyer, K. F.; Xi, S.; Mai, J. C.; Robbins, P. D.; Gadiparthi,
300 S.; Burke, N. a; Watkins, S. F.; Grandis, J. R. Targeted inhibition of Stat3 with a decoy
301 oligonucleotide abrogates head and neck cancer cell growth. *Proc. Natl. Acad. Sci. U. S. A.* **2003**, *100*,
302 4138–4143.

303 26. Sen, M.; Paul, K.; Freilino, M. L.; Li, H.; Li, C.; Johnson, D. E.; Wang, L.; Eiseman, J.; Grandis, J. R.
304 Systemic administration of a cyclic signal transducer and activator of transcription 3 (STAT3) decoy
305 oligonucleotide inhibits tumor growth without inducing toxicological effects. *Mol. Med.* **2014**, *20*,
306 46–56.

307 27. Sen, M.; Tosca, P. J.; Zwayer, C.; Ryan, M. J.; Johnson, J. D.; Knostman, K. A. B.; Giclas, P. C.;
308 Peggins, J. O.; Tomaszewski, J. E.; McMurray, T. P.; Li, C.; Leibowitz, M. S.; Ferris, R. L.; Gooding,
309 W. E.; Thomas, S. M.; Johnson, D. E.; Grandis, J. R. Lack of toxicity of a STAT3 decoy
310 oligonucleotide. *Cancer Chemother. Pharmacol.* **2009**, *63*, 983–995.

311 28. Xi, S.; Gooding, W. E.; Grandis, J. R. In vivo antitumor efficacy of STAT3 blockade using a

312 transcription factor decoy approach: implications for cancer therapy. *Oncogene* **2005**, *24*, 970–979.

313 29. Changyou, L.; Zang, Y.; Sen, M.; Leeman-Neill, R. J.; Man, D. S.; Grandis, J. R.; Johnson, D. E.

314 Bortezomib up-regulates activated signal transducer and activator of transcription-3 and synergizes

315 with inhibitors of signal transducer and activator of transcription-3 to promote head and neck

316 squamous cell carcinoma cell death. *Mol. Cancer Ther.* **2009**, *8*, 2211–2220.

317 30. Sen, M.; Thomas, S. M.; Kim, S.; Yeh, J. I.; Ferris, R. L.; Johnson, J. T.; Duvvuri, U.; Lee, J.; Sahu, N.;

318 Joyce, S.; Freilino, M. L.; Shi, H.; Li, C.; Ly, D.; Rapireddy, S.; Etter, J. P.; Li, P. K.; Wang, L.; Chiosea,

319 S.; Seethala, R. R.; Gooding, W. E.; Chen, X.; Kaminski, N.; Pandit, K.; Johnson, D. E.; Grandis, J. R.

320 First-in-human trial of a STAT3 decoy oligonucleotide in head and neck tumors: Implications for

321 cancer therapy. *Cancer Discov.* **2012**, *2*, 694–705.

322 31. Hecker, M.; Wagner, A. H. Transcription factor decoy technology: A therapeutic update. *Biochemical*

323 *Pharmacology*, **2017**, *144*, 29–34.

324 32. Winkler, J. Therapeutic oligonucleotides with polyethylene glycol modifications. *Future Med. Chem.*

325 **2015**, *7*, 1721–1731.

326 33. Higuchi, Y.; Furukawa, K.; Miyazawa, T.; Minakawa, N. Development of a new dumbbell-shaped

327 decoy DNA using a combination of the unnatural base pair ImO^N:NaNO and a CuAAC reaction.

328 *Bioconjug. Chem.* **2014**, *25*, 1360–1369.

329 34. Miyake, T.; Aoki, M.; Osako, M. K.; Shimamura, M.; Nakagami, H.; Morishita, R. Systemic

330 administration of ribbon-type decoy oligodeoxynucleotide against nuclear factor B and ets prevents

331 abdominal aortic aneurysm in rat model. *Mol. Ther.* **2011**, *19*, 181–187.

332 35. Hedvat, M.; Huszar, D.; Herrmann, A.; Gozgit, J. M.; Schroeder, A.; Sheehy, A.; Buetner, R.; Proia,

333 D.; Kowolik, C. M.; Xin, H.; Armstrong, B.; Bebernitz, G.; Weng, S.; Wang, L.; Ye, M.; McEachern,

334 K.; Chen, H.; Morosini, D.; Bell, K.; Alimzhanov, M.; Ioannidis, S.; McCoon, P.; Cao, Z. A.; Yu, H.;

335 Jove, R.; Zinda, M. The JAK2 Inhibitor AZD1480 Potently Blocks Stat3 Signaling and Oncogenesis in

336 Solid Tumors. *Cancer Cell* **2009**, *16*, 487–497.

337 36. Weinstein, I. B.; Joe, A. Oncogene addiction. *Cancer Research*, **2008**, *68*, 3077–3080.

338 37. Njatcha, C.; Farooqui, M.; Grandis, J. R.; Siegfried, J. M. Targeting the EGFR/STAT3 axis in NSCLC

339 with resistance to EGFR tyrosine kinase inhibitors using an oligonucleotide-based decoy. *Cancer*

340 *Res.* **2017**.

341 38. Yan, C.; Higgins, P. J. Drugging the undruggable: Transcription therapy for cancer. *Biochimica et*

342 *Biophysica Acta - Reviews on Cancer*, **2013**, *1835*, 76–85.

343 39. Morishita, R.; Gibbons, G. H.; Horiuchi, M.; Ellison, K. E.; Nakama, M.; Zhang, L.; Kaneda, Y.;

344 Ogihara, T.; Dzau, V. J. A gene therapy strategy using a transcription factor decoy of the E2F

345 binding site inhibits smooth muscle proliferation in vivo. *Proc. Natl. Acad. Sci. U. S. A.* **1995**, *92*,

346 5855–5859.

347 40. Conte, M. S.; Bandyk, D. F.; Clowes, A. W.; Moneta, G. L.; Seely, L.; Lorenz, T. J.; Namini, H.;

348 Hamdan, A. D.; Roddy, S. P.; Belkin, M.; Berceli, S. A.; DeMasi, R. J.; Samson, R. H.; Berman, S. S.

349 Results of PREVENT III: A multicenter, randomized trial of edifoligide for the prevention of vein

350 graft failure in lower extremity bypass surgery. *J. Vasc. Surg.* **2006**, *43*.

351 41. Alexander, J. H.; Hafley, G.; Harrington, R. A.; Peterson, E. D.; Ferguson, T. B.; Lorenz, T. J.; Goyal,

352 A.; Gibson, M.; Mack, M. J.; Gennevois, D.; Califf, R. M.; Kouchoukos, N. T.; PREVENT IV

353 Investigators. Efficacy and safety of edifoligide, an E2F transcription factor decoy, for prevention of

354 vein graft failure following coronary artery bypass graft surgery: PREVENT IV: a randomized

355 controlled trial. *JAMA* **2005**, *294*, 2446–2454.

356 42. Lopes, R. D.; Williams, J. B.; Mehta, R. H.; Reyes, E. M.; Hafley, G. E.; Allen, K. B.; MacK, M. J.;
357 Peterson, E. D.; Harrington, R. A.; Gibson, C. M.; Califff, R. M.; Kouchoukos, N. T.; Ferguson, T. B.;
358 Lorenz, T. J.; Alexander, J. H. Edifoligide and long-term outcomes after coronary artery bypass
359 grafting: PRoject of Ex-vivo Vein graft ENgineering via Transfection IV (PREVENT IV) 5-year
360 results. *Am. Heart J.* **2012**, *164*.

361 43. Cogoi, S.; Jakobsen, U.; Pedersen, E. B.; Vogel, S.; Xodo, L. E. Lipid-modified G4-decoy
362 oligonucleotide anchored to nanoparticles: Delivery and bioactivity in pancreatic cancer cells. *Sci.*
363 *Rep.* **2016**, *6*.

364 44. Tranter, M.; Liu, Y.; He, S.; Gulick, J.; Ren, X.; Robbins, J.; Jones, W. K.; Reineke, T. M. In vivo
365 delivery of nucleic acids via glycopolymers vehicles affords therapeutic infarct size reduction in
366 vivo. *Mol. Ther.* **2012**, *20*, 601–608.

367 45. AnGes MG, I. AnGes announces top-line results for Japanese Phase 3 Clinical Trial of NF-kappaB
368 decoy oligonucleotide for atopic dermatitis. *Press Release* **2016**.

369 46. Inagaki, H.; Suzuki, J.; Ogawa, M.; Taniyama, Y.; Morishita, R.; Isobe, M.
370 Ultrasound-microbubble-mediated NF-kappaB decoy transfection attenuates neointimal formation
371 after arterial injury in mice. *J. Vasc. Res.* **2006**, *43*, 12–18.

372 47. Kopechek, J. A.; Carson, A. R.; McTiernan, C. F.; Chen, X.; Hasjim, B.; Lavery, L.; Sen, M.; Grandis, J.
373 R.; Villanueva, F. S. Ultrasound targeted microbubble destruction-mediated delivery of a
374 transcription factor decoy inhibits STAT3 signaling and tumor growth. *Theranostics* **2015**, *5*, 1378–
375 1387.

376 48. Wahlestedt, C.; Salmi, P.; Good, L.; Kela, J.; Johnsson, T.; Hökfelt, T.; Broberger, C.; Porreca, F.; Lai,
377 J.; Ren, K.; Ossipov, M.; Koshkin, A.; Jakobsen, N.; Skou, J.; Oerum, H.; Jacobsen, M. H.; Wengel, J.
378 Potent and nontoxic antisense oligonucleotides containing locked nucleic acids. *Proc. Natl. Acad. Sci.*
379 *U. S. A.* **2000**, *97*, 5633–5638.